Decomposition of the Benzyl Radical: Quantum Chemical and Experimental (Shock Tube) Investigations of Reaction Pathways

Jeffrey Jones, George B. Bacskay, and John C. Mackie*

School of Chemistry, University of Sydney, NSW 2006, Australia

Received: April 28, 1997; In Final Form: June 20, 1997[⊗]

Decomposition of the benzyl radical at a range of temperatures, ∼1450−1650 K, has been investigated using *ab initio* quantum chemical and experimental (shock tube) techniques. Four possible decomposition mechanisms are considered: (a) via a norbornadienyl intermediate, (b) via a cycloheptatrienyl intermediate, (c) via direct ring opening, and (d) via a 6-methylenebicyclo[3.1.0]hex-3-en-2-yl (MBH) intermediate. On the basis of the quantum chemical calculations, mechanisms c and d are found to be the dominant reaction channels. A theoretically derived rate constant for the overall disappearance of benzyl is $k = 10^{16.6\pm0.3}$ exp(−97 ± 3 kcal mol^{-1}/*RT*) s^{-1}, in reasonable agreement with that obtained in previous studies. The experiments were carried out by shock heating benzyl bromide to temperatures between 1050 and 1650 K, followed by analysis of the spectral components of benzyl bromide, benzyl, and benzyl "fragments". The rate constants derived from these experiments by using a simple two-step kinetic model are in good agreement with the theoretical values.

Introduction

High-temperature decomposition studies of simple aromatic molecules containing the benzyl fragment are of importance to areas such as the mechanisms of soot formation and combustion of aromatics. Toluene is a compound whose decomposition kinetics have been studied extensively over the past two decades using a variety of techniques.[1−8] The overall mechanism of decomposition under conditions of high temperature and pressure has been the subject of considerable controversy, due partly to the uncertainty concerning the relative importance of the two primary dissociation pathways

$$C_7H_8 \rightarrow C_6H_5CH_2 + H \quad (1)$$

resulting in the formation of benzyl radicals, and

$$C_7H_8 \rightarrow C_6H_5 + CH_3 \quad (2)$$

where phenyl and methyl radicals are formed.

At first, on the basis of thermochemistry, reaction 1 was thought to govern the decomposition of toluene, but later it was found that the reverse reaction, i.e., the recombination of benzyl with hydrogen atoms, was very fast; hence, pathway 2 gained in importance, at least as far as the product distributions are concerned. Moreover, the exact nature of the subsequent decomposition of benzyl into fragments including C_5H_5, C_4H_4, C_3H_3, and C_2H_2 has not yet been clearly resolved, although an experimental rate constant for overall decomposition at temperatures greater than 1400 K has been reported[7] as $k = 10^{15.3}$ exp(−83.7 kcal mol^{-1}/*RT*) s^{-1}.

At lower temperatures (<1300 K) the primary mode of benzyl disappearance appears to be recombination to dibenzyl, followed by abstraction of H atoms from dibenzyl by benzyl radicals and subsequent H fission to form stilbene. Hippler et al.[7] have proposed a mechanism for this:

$$2C_6H_5CH_2 \rightarrow C_6H_5CH_2CH_2C_6H_5 \quad (3)$$

$$C_6H_5CH_2CH_2C_6H_5 + C_6H_5CH_2 \rightarrow C_6H_5CH_2CHC_6H_5 + C_6H_5CH_3 \quad (4)$$

$$C_6H_5CH_2CHC_6H_5 \rightarrow C_6H_5CHCHC_6H_5 + H \quad (5)$$

$$C_6H_5CH_2 + H \rightarrow C_6H_5CH_3 \quad (6)$$

With this mechanism they were successfully able to model the disappearance of benzyl at low temperatures as well as explaining the observed stoichiometric ratio of benzyl:H (approximately 1:1).

At temperatures greater than ∼1300 K, the overall decomposition mechanism apparently becomes more complex. The contribution of the "stilbene" pathway is significantly reduced in comparison with alternative routes that appear to assume greater importance. In this higher temperature regime, the main reactions in addition to reaction 6 may be summarized as follows:

$$C_6H_5CH_2 \rightarrow \text{fragments} + H \quad (7)$$

$$C_6H_5CH_2 \rightarrow C_5H_5 + C_2H_2 \quad (8)$$

$$C_6H_5CH_2 \rightarrow C_4H_4 + C_3H_3 \quad (9)$$

where the fragments in eq 7 include C_5H_5, C_4H_4, C_4H_3, C_3H_4, C_3H_3, and C_2H_2.

The rate constants for reactions 3 and 6 are now well established, and experiment suggests that the corresponding activation energy of (7) is around 83.7 kcal mol^{-1}. However, estimates of the rates of reactions 8 and 9 vary considerably, due to lack of knowledge of the specific nature of the products of decomposition and the likelihood that they are not elementary reactions. The complications introduced by the secondary processes lead to difficulties in the experimental determination of rate parameters for these reactions, so it is necessary to determine these parameters by kinetic modeling as well as on

[⊗] Abstract published in *Advance ACS Abstracts,* August 1, 1997.

S1089-5639(97)01419-9 CCC: $14.00

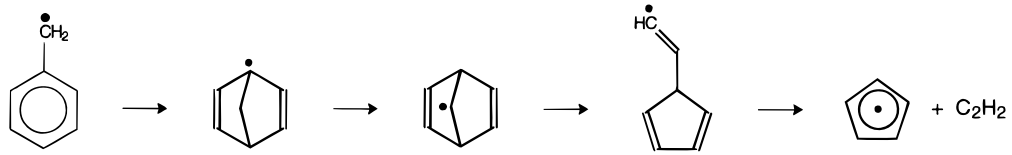

Figure 1. Decomposition of benzyl: the norbornadienyl pathway.

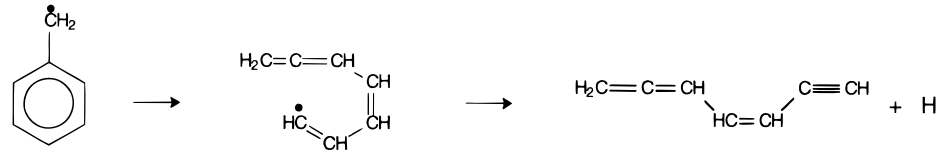

Figure 2. Decomposition of benzyl: the "chain" (ring-opening) pathway.

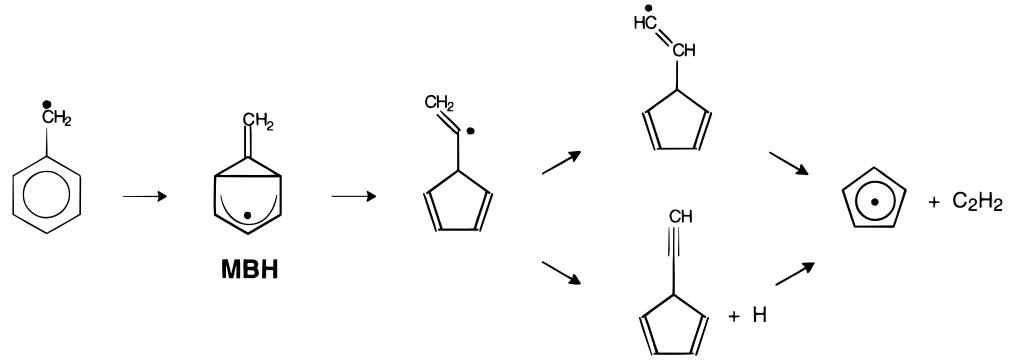

Figure 3. Decomposition of benzyl: the MBH "ring" pathway.

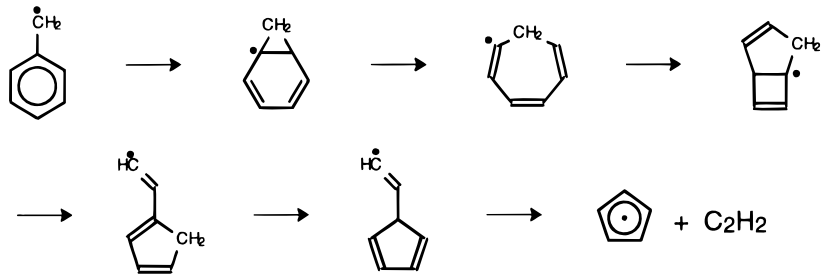

Figure 4. Decomposition of benzyl: the cycloheptatrienyl pathway.

thermochemical grounds. However, accurate estimates require a fairly detailed knowledge of the potential energy surfaces of the particular pathways. This is now achievable through the use of *ab initio* quantum chemical approaches, and the computation of potential energy surfaces is a primary objective of this study.

In a number of shock tube studies of the pyrolysis of toluene, cyclopentadiene and acetylene have been observed as products at temperatures between 1350 and 1900 K.[1,2,8] Colket et al.[8] postulated that these products come from a unimolecular decomposition of the benzyl radical with a moderately low activation energy (~70 kcal mol^{-1}). They proposed a mechanism involving the isomerization of benzyl to a norbornadienyl intermediate, followed by a direct cleavage, resulting in acetylene and a cyclopentadienyl radical (Figure 1). Experimental support for this mechanism was found by shock heating norbornadiene, which was found to yield toluene, cyclopentadiene, and acetylene as products. Other workers[6] have suggested that the activation energy associated with the above mechanism may be as low as 44.7 kcal mol^{-1}.

Braun-Unkhoff et al.[9] proposed two alternative mechanisms, based on their observations of the 1:1 ratio of benzyl to H atoms formed in the pyrolysis of benzyl iodide. Their first model, based on earlier work of Rao and Skinner[3] and termed the "chain model", entails a direct ring scission of benzyl followed by the loss of H from the open-chain C_7H_7 product to give a relatively stable C_7H_6 isomer (Figure 2). Subsequent fission and abstraction reactions involving this radical could then give rise to the smaller fragments observed. Their second proposal, the "ring model", following Benson's[10] suggestion, consists of an initial intramolecular rearrangement of the benzyl radical to a bicyclic intermediate, 6-methylenebicyclo[3.1.0]hex-3-en-2-yl (MBH). This could then isomerize to a vinyl−cyclopentadienyl radical and eventually form acetylene and cyclopentadiene (Figure 3). A mechanism analogous to this has been successfully used to describe the decomposition of the phenoxy radical.[11,12]

A fourth possible route to benzyl decomposition is shown in Figure 4. Again, it is initiated by an isomerization to a bicyclic intermediate (norcaradienyl), followed by the formation of a cycloheptatrienyl radical. A series of isomerizations follow, giving rise to the vinyl−cyclopentadienyl species shown. Although there are more steps involved in this pathway, the mechanism may be viable, provided the energy barriers are low.

It is relevant, at this point, to provide a brief review of our shock tube studies that were carried out on 2- and 3-picoline.[13,14] These compounds are aza-aromatic analogues of toluene and may therefore exhibit similar characteristics in their pyrolytic decomposition mechanisms. In addition, the presence of a nitrogen atom in the ring, serving as a marker, aids in differentiating between the various primary pathways. Experi-

mental results and kinetic modeling carried out on these molecules showed that the primary means of decomposition of the picolyl radicals (analogous to benzyl) is direct ring opening, followed by fission of the resulting open-chain radical into smaller fragments. Although molecular rearrangement mechanisms similar to those outlined above were considered in our picoline studies, none could successfully reproduce the observed kinetics nor explain the presence of some of the observed products.

Despite the large body of previous work that attempts to explain the decomposition of benzyl, there is still a considerable degree of uncertainty about the mechanism. The experiments have clearly shown that, due to the large degree of interaction between the product and intermediate species, it is difficult to resolve the contributions of the various proposed decomposition pathways.

In the present work, we examine the mechanisms discussed above, largely from a theoretical standpoint. Details of the potential energy surfaces, calculated by *ab initio* quantum chemical techniques, along with estimates of critical energies and Arrhenius frequency factors are presented and analyzed. In addition, we report the results of shock tube experiments using benzyl bromide as a source of benzyl radicals. Through the use of CCD/UV spectroscopy we are able to observe the growth and decay of intermediate species throughout the lifetime of the reaction and thus to estimate the overall rate of benzyl decomposition by utilizing a simple kinetic model. Consequently, we are able to assess the importance of the various reaction pathways.

Computational Section

The potential energy surfaces presented in this study were obtained using *ab initio* quantum chemical methods. Restricted Hartree−Fock (RHF) theory was employed initially to obtain equilibrium and transition state geometries, using 3-21G bases.[15] Most structures were then reoptimized using multiconfigurational SCF (MCSCF) theory in conjunction with the 3-21G basis, using the complete active space SCF (CASSCF) method of Roos et al.,[16] with 5−9 active electrons in 5−9 active orbitals. The vibrational frequencies were also calculated at the CASSCF/3-21G level and used (without scaling) to estimate zero-point corrections to the electronic energies. As a check on the accuracy of the 3-21G geometries, the structures of a few molecules were reoptimized at the CASSCF level using Dunning's cc-pVDZ basis.[17]

Single-point energy calculations were carried out at the optimized geometries using the complete active space second-order perturbation (CASPT2) method[18] in conjunction with the cc-pVDZ basis, with 3−5 active electrons in 3−5 active orbitals. In a few instances the energies were recalculated using the (single reference) projected MP4 (PUMP4) method and, as a test for basis set convergence, using PUMP2 with a 6-311G-(2df,p) basis.[19]

Using transition state theory in combination with the appropriate partition functions and critical energies obtained in the *ab initio* computations, theoretical estimates of the rate constants, defined in terms of the above quantities, were obtained for the key reactions in each decomposition scheme. Expected errors in the critical energy are obtained on the basis of the quantum chemical calculations. We estimate that the use of an all vibrations model for benzyl and its transition states could lead to an error of a factor of ∼2 in the *A* factors. Approximate rate constants for the disappearance of benzyl were then calculated using a steady state approach in cases where more than one reaction could be considered rate determining. Based on previous work,[14] the above methods are expected to yield estimates of the rate parameters to within 5−10% of the experimentally determined values.

The quantum chemical computations were carried out using the CADPAC,[20] SIRIUS,[21] ABACUS,[22] MOLCAS2,[23] and GAUSSIAN 94[24] programs implemented on IBM RS6000 and DEC alpha workstations.

Experimental Section

The experiments were carried out in this study using a single-pulse shock tube (SPST) with an internal diameter of 7.6 cm. Two sapphire windows fitted at the end of the shock tube permitted analysis through real time UV-absorption spectroscopy. The source, a xenon arc lamp (150 W), is focused through the windows onto the slit of a SPEX 270M monochromator which has a charged coupled device (CCD) chip located at its exit. The chip consists of a matrix of 512 × 512 pixels, each of which is capable of storing light intensity information. To enable multiple spectra to be taken during the reaction, the incident light is focused on the top 10 rows of the chip for a preset length of time (25 μs in this study). The charge is then shifted down into the next 10 rows of the unexposed region of the chip, taking a further total of 24 μs to do this. The top 10 rows are then reexposed, and the shifting procedure is repeated until the entire chip is full, for a total of 51 × 10 spectra. The spectral information contained in each set of 10 rows are summed and averaged using pixel binning. In this way, a series of 51 spectra could be taken at intervals of 49 μs, although in our experiments only 10−15 of these fell within the residence time of the reflected shocked gas and could be used for further analysis. The method of analysis will be described below.

Benzyl bromide (>98%, Merck) was used without further purification after degassing. Mixtures of benzyl bromide in argon were prepared in the reactor at concentrations of between 1×10^{-8} and 3×10^{-7} mol dm^{-3}. The conditions of the reflected shock increased these by approximately a factor of 4. The measurement of the incident and reflected shock velocities enabled the pressures and temperatures behind the reflected shock to be obtained. In this study, temperatures ranged from 1050 to 1650 K and pressures from 10 to 12 atm. Reaction residence times were between 550 and 900 μs, and the wavelength region examined is 270−330 nm.

Results

***Ab Initio* Potential Energy Surfaces.** The potential energy surfaces described previously (norbornadienyl, cycloheptatrienyl, ring-opening, and MBH pathways) are shown in Figures 5−8. The energies of each species are depicted relative to that calculated for benzyl, for which a heat of formation of 47.8 kcal mol^{-1} was assumed.[25] Although other workers[9,26] have suggested that this value may be too low by as much as 4 kcal mol^{-1}, the relative energies quoted here are unaffected by such a correction. Where relevant, alternative pathways are shown, while others are excluded because of the large critical energies involved. Arrhenius rate parameters were calculated from the *ab initio* data for the critical reactions of each of the four schemes; these are given in Table 1.

On the basis of the computed critical energies and frequency factors, the ring-opening reaction **1** → **12** → **13** and hydrogen fission reaction **16** → **18** → **19** are expected to be the most important in determining the overall rate of decomposition. Therefore, as a check on the accuracy of the CASPT2/cc-pVDZ calculations, a series of further computations were carried out at different levels of theory as well as with larger basis sets.

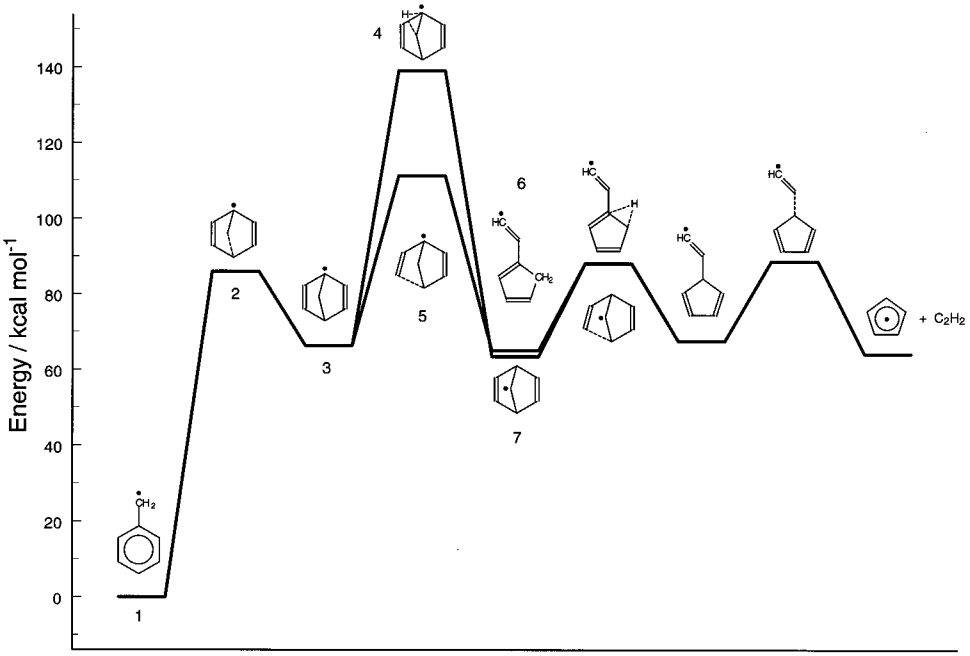

Figure 5. Decomposition of benzyl: potential energy surface for the norbornadienyl pathway. Energies at 0 K are relative to benzyl.

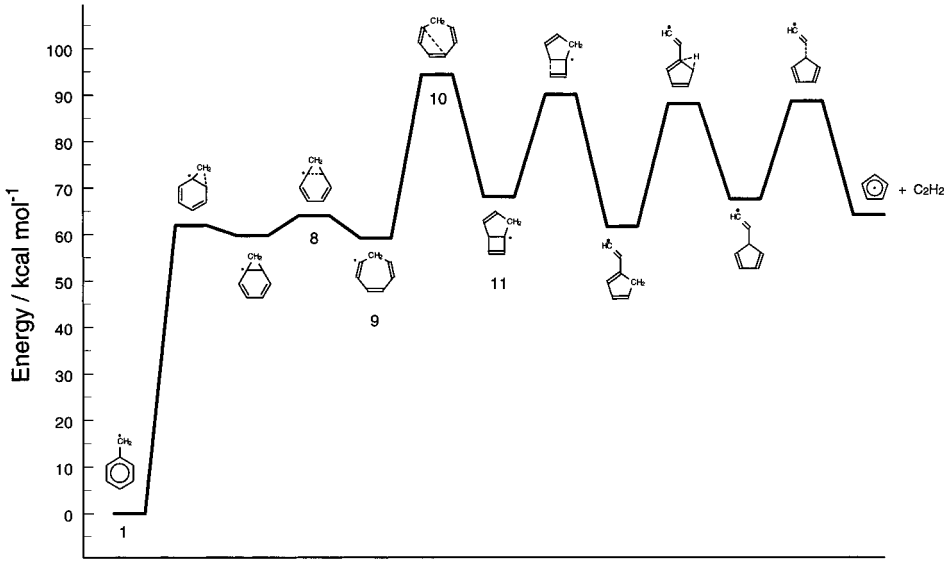

Figure 6. Decomposition of benzyl: potential energy surface for the cycloheptatrienyl pathway. Energies at 0 K are relative to benzyl.

In the case of the ring-opening reaction, the reverse barrier, when calculated at the CASSCF level, is very small (∼2 kcal mol^{-1}). At the CASSCF geometries the CASPT2 energies of **12** and **13** are such as to suggest that a barrier may not exist at all. Our approach to resolving this dilemma is a conservative one: use the CASSCF geometry and frequencies for the calculation of the frequency factor and, similarly, use the CASSCF/cc-pVDZ energies to compute the reverse barrier height.

To establish the reliability of the forward barrier, viz. critical energy of the ring-opening reaction, a series of additional computations were carried out on the reactant **1** and product **13**. The results are summarized in Table 2. Reoptimization of the geometry at the CASSCF/cc-pVDZ level has a small effect on the energy (∼1.6 kcal mol^{-1} at the CASPT2 level), validating the use of the 3-21G basis for geometries. Electron correlation is clearly very important: the CASSCF and projected unrestricted Hartree−Fock (PUHF) estimates of the relative energy are too low by up to ∼17 kcal mol^{-1}. The projected MP2 (PUMP2) and MP4 (PUMP4) results are close to each other and to the CASPT2 values, suggesting that the projected Møller−Plesset perturbation series has good convergence characteristics. Enlarging the valence part of the basis to triple zeta and adding additional polarization functions on the C atoms (2df) results in an energy lowering by just 1.3 kcal mol^{-1}. Consequently, the best estimate for the energy of the reaction (based on the CASPT2(5/5)/cc-pVDZ//CASSCF(9/9)/cc-pVDZ and PUMP2 results) is 94.9 kcal mol^{-1}. Adding on the previously computed value for the reverse barrier (2.1 kcal mol^{-1}) results in a critical energy of reaction of 97.0 kcal mol^{-1}. On the basis of our computed energies, we suggest a conservative estimate of the error in the critical energy as ±3 kcal mol^{-1}.

In the case of the transition state **18** a similar set of calculations were carried out, the results being summarized in Table 3. Correcting the CASPT2(5/5)/cc-pVDZ//CASSCF(9/9)/3-21G energies for basis set effects (which again are seen to be small), our best estimate for the energy of **18** is 98.3 kcal mol^{-1} above benzyl, with an estimated error of ±3 kcal mol^{-1} in this case also.

Norbornadienyl Pathway. The norbornadienyl pathway is

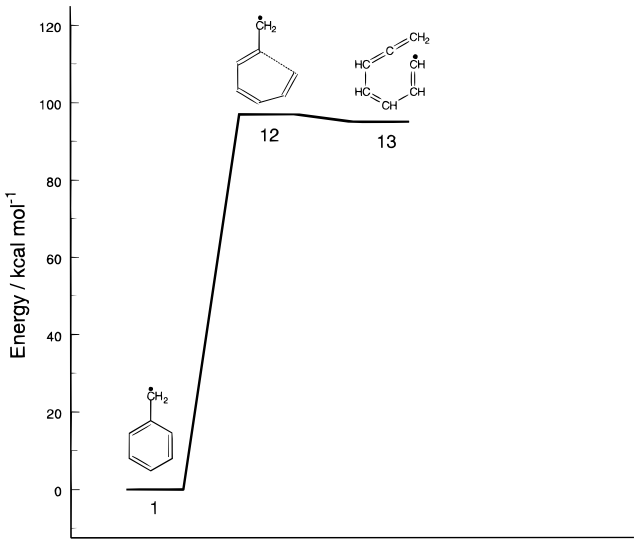

Figure 7. Decomposition of benzyl: potential energy surface for the ring-opening pathway. Energies at 0 K are relative to benzyl.

TABLE 1: Arrhenius Frequency Factors and Critical Energies (in kcal mol^{-1}) for Selected Reactions in the Different Reaction Pathways

mechanism	reaction[a]	log A[b]	$\Delta E^{\ddagger}_c$
norbornadienyl	1 → 2 → 3	13.1	86.0 (86.0)[c,d]
norbornadienyl	3 → 4 → 7	14.0	72.8 (139.1)
norbornadienyl	3 → 5 → 6	14.1	44.9 (111.3)
cycloheptatrienyl	1 → 8 → 9	13.1	64.0 (64.0)
cycloheptatrienyl	9 → 10 → 11	13.2	35.2 (94.4)
ring opening	1 → 12 → 13	16.1	97.0 (97.0)
MBH	1 → 15 → 16	14.3	74.9 (74.9)
MBH	16 → 17 → 20	13.9	44.8 (109.9)
MBH	16 → 18 → 19	15.5	33.8 (99.0)

[a] Labeling of species as indicated in Figures 5−8. [b] Computed at 1500 K. [c] $\Delta E^{\ddagger}_c$(r→c‡→p) = E(c‡) − E(r). [d] $\Delta E^{\ddagger}_c$(relative to benzyl) = E(c‡) − E(benzyl) in parentheses.

clearly unfavorable when compared with the MBH pathway as a route to cyclopentadiene and acetylene (Figures 1 and 5). As shown in Figure 5, the critical energy at 0 K for the first step (the formation of the norbornadienyl radical) was calculated as

TABLE 2: Energy (in kcal mol^{-1}) of the Open Chain Radical (10) Relative to Benzyl Using Different Levels of Theory and Basis Sets[a]

energy	geometry	ΔE[a]
CASSCF(7/7)/3-21G	CASSCF(7/7)/3-21G	85.31
CASPT2(3/3)/cc-pVDZ	CASSCF(7/7)/3-21G	101.50
CASPT2(5/5)/cc-pVDZ	CASSCF(7/7)/3-21G	100.40
CASSCF(9/9)/cc-pVDZ	CASSCF(9/9)/cc-pVDZ	81.30
CASPT2(3/3)/cc-pVDZ	CASSCF(9/9)/cc-pVDZ	98.9
CASPT2(5/5)/cc-pVDZ	CASSCF(9/9)/cc-pVDZ	96.2
PUHF/cc-pVDZ	CASSCF(9/9)/cc-pVDZ	83.37
PUMP2/cc-pVDZ	CASSCF(9/9)/cc-pVDZ	94.27
PUMP4/cc-pVDZ	CASSCF(9/9)/cc-pVDZ	95.03
B3LYP/cc-pVDZ	CASSCF(9/9)/cc-pVDZ	90.60
PUHF/6−311G(2df,p)	CASSCF(9/9)/cc-pVDZ	81.74
PUMP2/6−311G(2df,p)	CASSCF(9/9)/cc-pVDZ	92.98

[a] The energies (ΔE) include zero-point vibrational corrections.

TABLE 3: Energy (in kcal mol^{-1}) of the Acetyl−Cyclopentadiene Transition State (18) (Relative to Benzyl) Obtained at Different Levels of Theory and Basis Sets at the CASSCF(9/9)/3-21G Geometry

energy	$\Delta E_c^{\ddagger}$
CASSCF(9/9)/3-21G	70.05
CASPT2(5/5)/cc-pVDZ	99.35
PUHF/cc-pVDZ	125.22
PUMP2/cc-pVDZ	98.52
PUMP4/cc-pVDZ	95.65
PUHF/6−311G(2df,p)	124.63
PUMP2/6−311G(2df,p)	97.43

[a] The energies ΔE include zero-point vibrational corrections.

∼86 kcal mol^{-1}, placing it ∼15 kcal mol^{-1} higher than the activation energy estimated by Colket et al.[8] for this pathway. However, the main problem with this mechanism is that both the subsequent H transfer and ring-opening steps, involving the transition states **4** and **5**, respectively, require additional energies of 55 and 25 kcal mol^{-1} to proceed. These values, combined with the relatively low A factors associated with these types of isomerizations (see Table 1), lead us to conclude that the norbornadienyl route to benzyl decomposition is likely to be relatively unimportant, although some norbornadiene will probably form. The possibility of a concerted, one-step reaction of

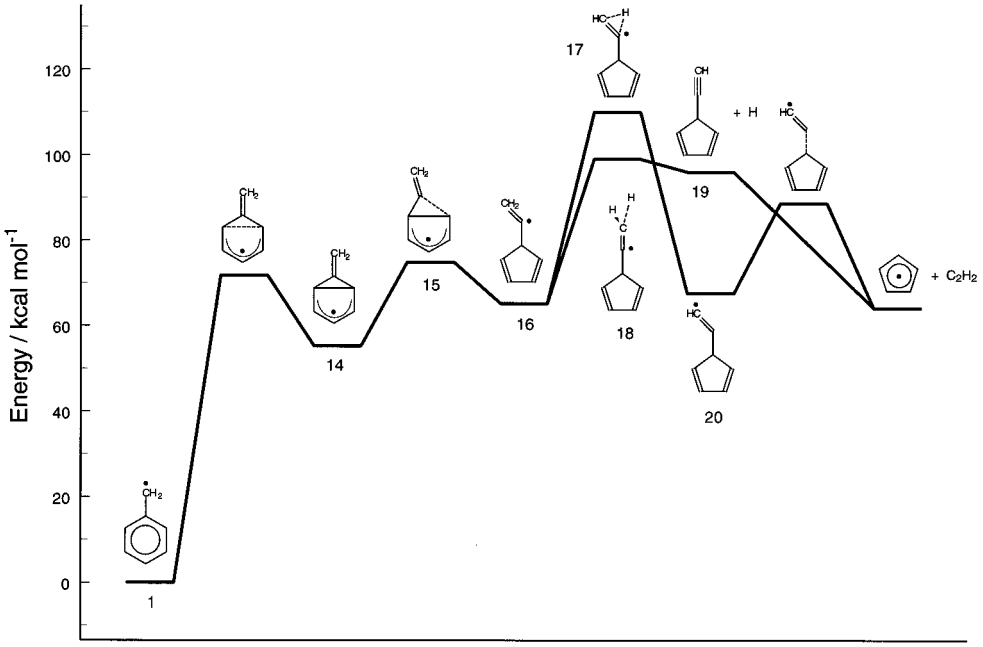

Figure 8. Decomposition of benzyl: potential energy surface for the 6-methylenebicyclo[3.1.0]hex-3-en-2-yl (MBH) "ring" pathway. Energies at 0 K are relative to benzyl.

the norbornadienyl intermediate **3** to give acetylene and a 1,2-H cyclopentadienyl isomer was also considered. However, according to our computations, the 1,2-H isomer itself has an absolute energy some 30 kcal mol^{-1} higher than that of cyclopentadienyl, placing the barrier to this process at a minimum of ~95 kcal mol^{-1}.

Cycloheptatrienyl Pathway. As expected, the initial benzyl−norcaradienyl−cycloheptatrienyl rearrangement (Figures 4 and 6) proceeds with relative ease, the highest critical energy barrier encountered being only ~64 kcal mol^{-1} with an associated Arrhenius preexponential factor of $10^{13.0}$ s^{-1}. This is in accordance with a number of experiments that report this rearrangement to be very rapid.[27] It also indicates that small amounts of cycloheptatriene may be present in pyrolyses of toluene or other benzyl precursors. To proceed further along this pathway toward cyclopentadienyl/acetylene formation requires an overall barrier of 94.4 kcal mol^{-1} for the collapse of the seven-membered ring to give a bicyclic intermediate **11** via transition state **10**. The *A* factor for this step was calculated as $10^{13.2}$ s^{-1}, which suggests that the overall rate for this process is likely to be too low to explain the overall disappearance of benzyl and the corresponding appearance of cyclopentadiene and acetylene.

Ring-Opening Pathway. The direct ring opening (Figures 2 and 7) as a primary means of benzyl decomposition has not been given serious consideration on the grounds that the activation energy is likely to be too high to explain the observed products at low temperatures. However, such ring-opening processes are also typically associated with transition states that closely resemble the open-chain product, giving rise to frequency factors larger than 10^{15} s^{-1}, which may well yield a sufficiently high overall rate to explain some of the experimental observations, despite the high activation energy. Rao and Skinner[3] were actually able to model benzyl decomposition using this mechanism.

The most likely fate of the open-chain radical produced from this reaction is to fission into the smaller open-chain fragments C_5H_5, C_4H_4, C_4H_3, C_3H_4, C_3H_3, and C_2H_2. While cyclization of the C_5H_5 radical may lead to the formation of some cyclopentadiene, it is more likely to undergo further fission into C_3H_3 and C_2H_2. A more direct route to cyclopentadiene formation, viz. the MBH pathway, is discussed in the next section.

Our calculated values for the frequency factor and critical energy of the ring-opening reaction are $10^{16.1\pm0.3}$ s^{-1} and 97 ± 3 kcal mol^{-1}, respectively. This energy is probably an upper limit, and the resulting rate of decomposition is therefore slightly lower than that reported by Hippler et al.[7] On the other hand, the disagreement may also indicate the possible presence of other mechanisms of decomposition that contribute to the experimentally observed rate.

Our computations suggest that the ring-opening mechanism would account for a significant portion of the decomposition of benzyl at temperatures greater than 1300 K and should be the primary source of the stable products C_4H_3 and C_3H_4 (to a lesser extent C_2H_2) and the radicals C_4H_4 and C_3H_3.

6-Methylenebicyclo[3.1.0]hex-3-en-2-yl Pathway. The MBH route (Figures 3 and 8), analogous to that for the decomposition of the phenoxy radical, involves the formation of the MBH intermediate **14**. For the initial four steps of this pathway, the maximum energy barrier was calculated to be ~75 kcal mol^{-1}. This is significantly lower than the value found for the first steps of the norbornadienyl pathway and is incidentally quite similar to the value used by Colket et al.[8] in their model. It is some 18 kcal mol^{-1} higher than the critical energy calculated for the analogous steps for the loss of CO from the phenoxy radical[11,12] at a comparable level of theory.

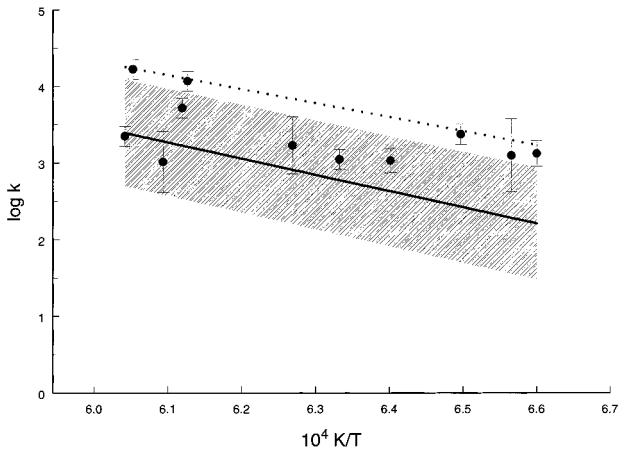

Figure 9. Comparison of rate constants for the dissociation of the benzyl radical in the temperature range 1500−1650 K: (—) theoretical values (this work); (●) experiment (this work); (•••) experiment (ref 7). The shading indicates the range of uncertainty associated with the theoretical prediction.

However, as may be seen from Figure 8, the unimolecular pathway includes a 1,2-H shift in **16**, and the transition state **17** corresponds to a prohibitively high barrier (see also Table 1). Consequently, it is unlikely that a route to acetylene and cyclopentadiene occurs by a completely unimolecular mechanism. The alternative, more feasible mechanism, involves the C−H bond breaking reaction **16** → **18** → **19**, followed by H addition to displace acetylene as proposed by Braun-Unkhoff et al.[9] We estimate the maximum barrier height to this process to be ~99 kcal mol^{-1}, comparable with that calculated for ring opening.

Rate Parameters for the Overall Reaction. In order to obtain an estimate of the decomposition of benzyl through the MBH pathway, we must separate it into two steps. The first is the isomerization to the vinyl−cyclopentadienyl intermediate **16** for which, using transition state theory, we calculate a value of $k_{1f} = 10^{14.3} \exp(-72 \text{ kcal mol}^{-1}/RT)$ s^{-1} from the *ab initio* data on transition state **18** at 1500 K. The reverse rate constant has a value of $k_{1r} = 10^{12.74} \exp(-8.7 \text{ kcal mol}^{-1}/RT)$ s^{-1}. The subsequent H-fission step (via **18**) has a calculated rate constant of $k_{2f} = 10^{15.0} \exp(-35.5 \text{ kcal mol}^{-1}/RT)$ s^{-1}. Using a steady state approximation, we obtain an expression for the rate of decomposition via the MBH pathway

$$k_{\text{dis,MBH}} = k_{1f}k_{2f}/(k_{1r} + k_{2f})$$

from which we obtain (via a least-squares fit) the rate constant for benzyl disappearance through this pathway as $k_{\text{dis,MBH}} = 10^{16.4} \exp(-97.4 \text{ kcal mol}^{-1}/RT)$ s^{-1}. Interestingly, this value is very similar to that obtained for the ring-opening (r-o) pathway, suggesting a close competition between the two mechanisms. Taking this into account, the overall rate for the decomposition of benzyl at $T > 1300$ K can therefore be expressed as

$$k = k_{\text{MBH}} + k_{\text{r-o}}$$
$$\cong 10^{16.6\pm0.3} \exp(-97 \pm 3 \text{ kcal mol}^{-1}/RT) \text{ s}^{-1} \qquad (10)$$

This result, in the form of an Arrhenius plot, is shown in Figure 9, where the shaded areas indicate the estimated errors in our calculations. The predicted rate constant is consistent

with the experimental results of this work as well as with the results of Hippler et al.[7]

Experimental Results. To interpret the UV spectra derived from our shock tube experiments, the following procedure was carried out. For each run, a series of 10−15 useful spectra, i.e., those obtained during the residence time of the reaction, were analyzed using the SPECFIT 2.10 program.[28] The program makes use of the factor analysis technique to deconvolute each spectral set into eigenvectors, consisting of noise and distinct spectral components. This permits us to observe and model the growth and decay of reaction intermediates and fragments throughout the course of the reaction. It has the advantage over conventional spectral analysis techniques in that it is 3-dimensional with respect to absorbance, wavelength range, and time. A simple model, described below, was employed to calculate kinetic parameters for the data using the Marquardt least-squares fitting technique. The input required species concentrations and rates for "fixed" reactions, i.e., reactions where rate constants are not varied in the fitting process. The limitations of this technique include the necessity of using very small kinetic models, as well as problems with time resolution above certain rates of reaction.

We carried out a series of experiments at temperatures below that required for the onset of benzyl decay (<1150 K) in order to determine the accuracy of the above method. At these temperatures, we assumed that benzyl bromide will form benzyl radicals, which may subsequently recombine to give dibenzyl. The model employed reflected this:

$$\mathrm{BzBr} \leftrightarrow \mathrm{Bz} + \mathrm{Br} \qquad (11)$$

$$2\mathrm{Bz} \rightarrow \text{dibenzyl} \qquad (3)$$

The forward rate constant of (11) was allowed to vary, and the reverse rate constant was calculated from the equilibrium constant for the reaction. The rate constant of (3) was fixed at a value[29] of 3×10^{12} cm^3 mol^{-1} s^{-1}. The validity of this simple mechanism was tested against a more detailed scheme, including the following reactions: three-body recombination of Br atoms to give the bromine molecule (Br_2); abstraction by the Br radical of a methylene hydrogen from dibenzyl to produce the C_6H_5-$CH{\cdot}CH_2C_6H_5$ radical and its subsequent fission of an H atom to form stilbene. H atom abstraction reactions from benzyl bromide and dibenzyl were also included. Rate constants for these reactions were either estimated from analogous reactions or taken from the National Institute of Standards and Technology kinetics database.[30] It was found, however, that the inclusion of these extra reactions had no significant effect on the concentration of the benzyl radical. Omission of the reverse reaction −11 has the effect of lowering the apparent rate constant for k_{11} by about 30%.

Factor analysis performed on the low-temperature spectra gave two components with different temporal behaviors corresponding to the known spectra of benzyl bromide and benzyl radicals (Figure 10). The evolution with time of the spectra at 1128 K may be observed in Figure 11. Although the spectra shown were not deconvoluted, the progression from benzyl bromide to benzyl can be clearly seen. The presence of stilbene, a further decay product of dibenzyl, was not observed, due to the short residence times as well as the low temperatures of the reactions. At the low initial concentrations of benzyl bromide, measurement of this initial concentration (by gas chromatography) was not sufficiently accurate for the determination of precise Arrhenius parameters for the dissociation of benzyl bromide. Our estimate of the rate constant is generally lower by a factor of 1.5−2 than that of Swarc et al.,[31] who obtained

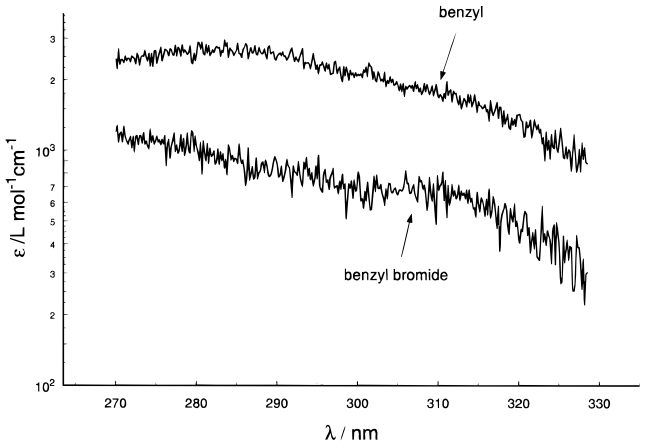

Figure 10. Absorption spectra of benzyl bromide and benzyl radicals at 1128 K.

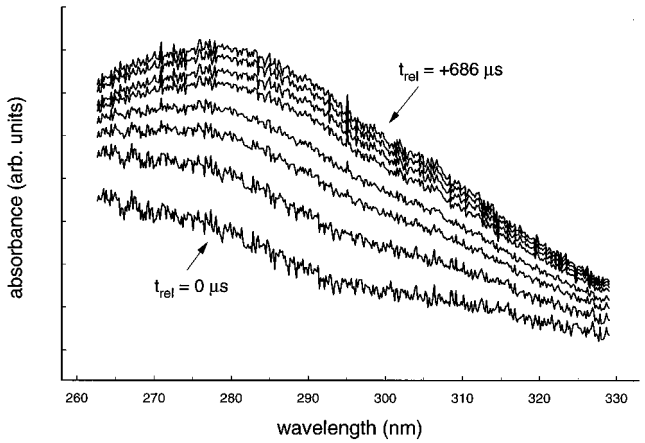

Figure 11. Evolution with time of benzyl radicals from benzyl bromide at 1128 K. The spectra shown are taken at intervals of 98 μs, with the first ($t_{rel} = 0$ μs) occurring some 25 μs after the reflected shock front.

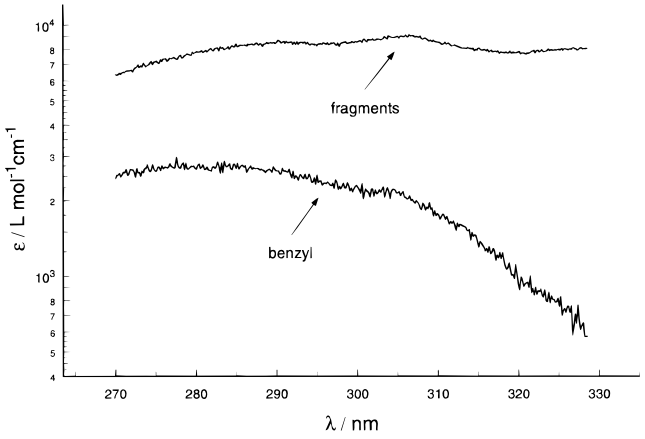

Figure 12. Absorption spectra of benzyl radicals and "benzyl fragments" at 1655 K.

a value (for reaction 11) of $k = 10^{13}$ exp(−50.5 ± 2 kcal mol^{-1}/RT) s^{-1}.

A series of higher temperature runs were then carried out between 1450 and 1650 K. Analytical problems were encountered outside these temperature ranges—we could only observe one spectral component below 1450 K (the benzyl radical), and the time resolution of the spectrometer was not fast enough above 1650 K to measure the larger rate constants expected. The spectral components corresponding to the benzyl radical and the fragments are displayed in Figure 12. On the basis of the similarity of the two high- and low-temperature benzyl

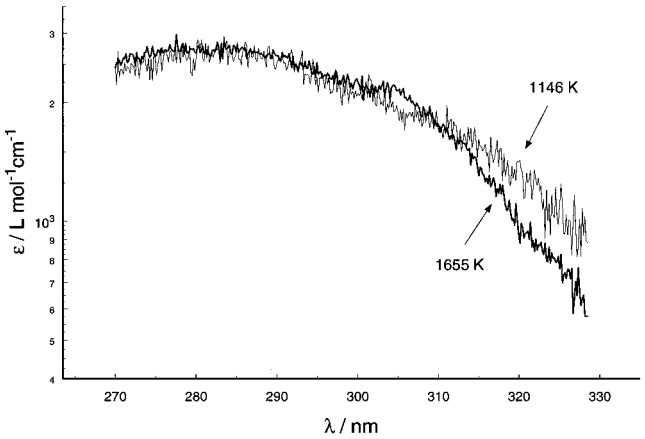

Figure 13. Comparison between the benzyl radical spectra taken at 1146 and 1655 K.

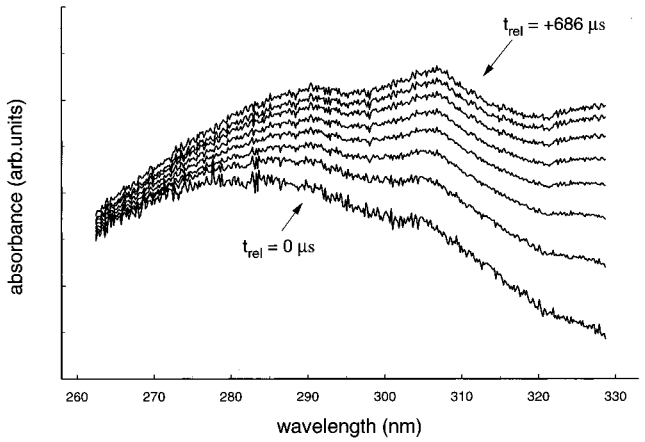

Figure 14. Evolution with time of benzyl fragments from benzyl radicals at 1655 K. The spectra shown are spaced at 98 μs, with the first ($t_{rel} = 0$ μs) occurring some 25 μs after the reflected shock.

spectra shown in Figure 13, we are confident that we have correctly assigned the spectral components observed in the benzyl bromide system. Figure 14 shows the evolution of the spectra for a typical run at the higher end of the temperature range. The first spectrum, approximately 25 μs after the reflected shock arrives ($t_{rel} = 0$ μs), corresponds primarily to the benzyl radical. Over the residence time of the reaction, the formation of the "fragments" spectrum may clearly be observed.

The above results were modeled kinetically, again using a two-step scheme:

$$\text{Bz} \rightarrow \text{fragments} \qquad (12)$$

$$2\text{Bz} \rightarrow \text{dibenzyl} \qquad (3)$$

It was assumed that at the onset of reaction all of the benzyl bromide was entirely converted to benzyl radicals at the temperatures studied. As before, the rate constant of (3) was fixed at 3×10^{12} cm^3 mol^{-1} s^{-1} and that of (12) allowed to vary. The individual rate data for k_{12} obtained from this model are shown in Figure 9, along with plots based on the rate of benzyl disappearance as determined by Hippler et al.[7] and the theoretical rate constant derived in this work. Again, the relative scatter of our experimental data makes it difficult to derive an sufficiently accurate overall rate constant for the disappearance of benzyl; however, all the data lie within or close to the error bounds associated with the theoretical rate, while being somewhat lower than the values reported by Hippler et al.[7] We believe that our proposed mechanism and the associated theoretically derived overall rate constant, k (eq 10), provide an adequate explanation of the rates of benzyl decomposition reported here as well as by others.[3,7,9]

In summary, therefore, having considered several mechanisms, it appears that the bicyclic 6-methylenebicyclo[3.1.0]-hex-3-en-2-yl (MBH) pathway is the most favorable for the formation of cyclopentadiene, while the ring-opening mechanism accounts for the other major products of benzyl decomposition. The overall rate constant for the disappearance of benzyl at temperatures greater than ~1450 K can thus be expressed as the sum of the two processes that leads to

$$k = 10^{16.6\pm0.3} \exp(-97 \pm 3 \text{ kcal mol}^{-1}/RT) \text{ s}^{-1} \qquad (10)$$

Conclusions

The decomposition of the benzyl radical at temperatures ranging from ~1450 to ~1650 K has been investigated using both theoretical and experimental approaches. Of the four alternative mechanisms examined, two were found to be dominant and equally feasible on the basis of our *ab initio* quantum chemical calculations. Direct ring scission into an open-chain C_7H_7 species followed by further fission provides an adequate explanation for the formation of the fragments C_4H_4, C_4H_3, C_3H_4, C_3H_3, and C_2H_2 that are observed as products. A rate for this process was estimated at $k_{r-o} = 10^{16.6} \exp(-97$ kcal mol$^{-1}/RT)$ s^{-1}. The second pathway, proceeding via the formation of the 6-methylenebicyclo[3.1.0]hex-3-en-2-yl (MBH) intermediate, appears to be a more direct route, however, to the formation of cyclopentadiene. We estimate the rate constant for dissociation through this mechanism as $k_{MBH} = 10^{16.4}$ exp(−97.4 kcal mol$^{-1}/RT)$ s^{-1}. When combined into an overall rate of disappearance of benzyl (10), we obtain a value that is in good agreement with experiments reported in this work and those of other workers.[3,7,9] The similarity of the two rate constants indicates that each pathway is approximately of equal importance in the decomposition of the benzyl radical, helping to clarify some of the uncertainties that have been associated with this process.

Acknowledgment. We thank Professors Sture Nordholm (Göteborg University) and Jürgen Troe (Göttingen University) for their helpful discussions. The financial support of the Australian Research Council Institutional Grants is gratefully acknowledged.

References and Notes

(1) Szwarc, M. *J. Chem. Phys.* **1948**, *16*, 128.
(2) Smith, R. D. *J. Phys. Chem.* **1979**, *83*, 1553.
(3) Rao, V. S.; Skinner, G. B. *Symp. (Int.) Combust., (Proc.), 21st* **1986**, 809.
(4) Pamidimukkala, K. M.; Kern, R. D.; Patel, M. R.; Wei, H. C.; Kiefer, J. H. *J. Phys. Chem.* **1987**, *91*, 2148.
(5) Brouwer, L. D.; Müller-Markgraf, W.; Troe, J. *J. Phys. Chem.* **1988**, *92*, 4905.
(6) Braun-Unkhoff, M.; Frank, P.; Just, Th. *Symp. (Int.) Combust., (Proc.), 22nd* **1988**, 1053.
(7) Hippler, H.; Reihs, C.; Troe, J. *Z. Phys. Chem. (Munich)* **1990**, *167*, 1.
(8) Colket, M. B.; Seery, D. J. *Symp. (Int.) Combust., (Proc.), 25th* **1994**, 883.
(9) Braun-Unkhoff, M.; Frank, P.; Just, Th. *Ber. Bunsen-Ges. Phys. Chem.* **1990**, *94*, 1417.
(10) Benson, S. W. *Symp. (Int.) Combust., (Proc.), 21st* **1986**, 813.
(11) Olivella, S.; Solé, A.; García-Raso, A. *J. Phys. Chem.* **1995**, *99*, 10549.
(12) Liu, R.; Morokuma, K.; Mebel, A.; Lin, M. C. *J. Phys. Chem.* **1996**, *100*, 9314.
(13) Doughty, A.; Mackie, J. C. *J. Phys. Chem.* **1992**, *96*, 10339.
(14) Jones, J.; Bacskay, G. B.; Mackie, J. C. *Isr. J. Chem.* **1996**, *36*, 239.
(15) Binkley, J. S.; Pople, J. A.; Hehre, W. J. *J. Am. Chem. Soc.* **1980**, *102*, 939.

(16) Roos, B. O.; Taylor, P. R.; Siegbahn, P. E. M. *Chem. Phys.* **1980**, *48*, 157.
(17) Dunning, T. H. *J. Chem. Phys.* **1989**, *90*, 1007.
(18) Andersson, K.; Roos, B. O. *Int. J. Quantum Chem.* **1993**, *45*, 591.
(19) Krishnan, R.; Binkley, J. S.; Seeger, R.; Pople, J. A. *J. Chem. Phys.* **1980**, *72*, 4244.
(20) CADPAC 5.0: The Cambridge Analytical Derivatives Package Issue 5.0, Cambridge, 1992. A suite of quantum chemistry programs developed by R. D. Amos with contributions from R. L. Alberts, J. S. Andrews, S. M. Calwell, N. C. Handy, D. Jayatilaka, P. J. Knowles, R. Kobayashi, N. Koga, K. E. Laidig, P. E. Malsen, C. W. Murray, J. E. Rice, J. Sanz, E. D. Simandiras, A. J. Stone, and M.-D. Su.
(21) Jensen, H. J.; Ågren, H.; Olsen, J. SIRIUS MCSCF program.
(22) Helgaker, T.; Jensen, H. J.; Jørgensen, P.; Olsen, J.; Taylor, P. R. ABACUS MCSCF energy derivatives program.
(23) Andersson, K.; Blomberg, M. R. A.; Fülscher, M. P.; Kellö, V.; Lindh, R.; Malmquist, P.-Å; Noga, J.; Olsen, J.; Roos, B. O.; Sadlej, A. J.; Siegbahn, P. E. M.; Urban, M.; Widmark, P.-O. *MOLCAS version 2*; University of Lund: Lund, Sweden, 1991.
(24) *Gaussian 94* (Revision A.1): Frisch, M. J.; Trucks, G. W.; Schlegel, H. B.; Gill, P. M. W.; Johnson, B. G.; Robb, M. A.; Cheeseman, J. R.; Keith, T. A.; Petersson, G. A.; Montgomery, J. A.; Raghavachari, K.; Al-Laham, M. A.; Zakrzewski, V. G.; Ortiz, J. V.; Foresman, J. B.; Cioslowski, J.; Stefanov, B. B.; Nanayakkara, A.; Challacombe, M.; Peng, C. Y.; Ayala, P. Y.; Chen, W.; Wong, M. W.; Andres, J. L.; Replogle, E. S.; Gomperts, R.; Martin, R. L.; Fox, D. J.; Binkley, J. S.; Defrees, D. J.; Baker, J.; Stewart, J. P.; Head-Gordon, M.; Gonzalez, C.; Pople, J. A. Gaussian, Inc., Pittsburgh, PA, 1995.
(25) McMillen, D. E.; Golden, D. M. *Annu. Rev. Phys. Chem.* **1982**, *33*, 493.
(26) Hippler, H.; Troe, J. *J. Phys. Chem.* **1990**, *94*, 3803.
(27) (a) Maier, G. *Angew. Chem., Int. Ed. Engl.* **1967**, *6*, 402. (b) Vogel, E.; Wiedemann, W.; Roth, H. D.; Eimer, J.; Günther, H. *Leibigs Ann. Chem.* **1972**, *759*, 1. (c) Warner, P. M.; Lu, S.-L *J. Am. Chem. Soc.* **1980**, *102*, 331; **1973**, *95*, 5099. (d) Rubin, M. B. *J. Am. Chem. Soc.* **1981**, *103*, 7791.
(28) Binstead, R. A.; Zuberbühler, A. D. SPECFIT version 2.1, A program for global least-squares fitting of equilibrium and kinetic systems, Spectrum Software Associates, Chapel Hill, NC, 1993−4.
(29) Müller-Markgraf, W.; Troe, J. *J. Phys. Chem.* **1988**, *92*, 4899.
(30) Mallard, W. G.; Westley, F.; Herron, J. T.; Hampson, R. F.; Frizzel, D. H. *NIST Chemical Kinetics Database, Ver 5.0*; NIST Standard Reference Data; NIST: Gaithersberg, MD, 1993.
(31) Swarc, M.; Ghosh, B. N.; Sehon, A. H. *J. Chem. Phys.* **1950**, *18*, 1142.